Electronic Supplementary Material (ESI) for Dalton Transactions.

Supporting Information

A 3D heteropolyoxoniobate framework based on heart-shaped {$Te_2Nb_{19}O_{60}$} clusters with proton conduction property

Ping-Xin Wu, Yue Han, Yu-Jin Lin, Yan-Qiong Sun* and Shou-Tian Zheng*

[a] *Fujian Provincial Key Laboratory of Advanced Inorganic Oxygenated-Materials, College of Chemistry, Fuzhou University, Fuzhou, Fujian 350108, China.*

This file includes:

Section S1 Synthesis and Methods

Materials and General methods：$K_7H(Nb_6O_{19})\cdot13H_2O$ was synthesized on the basis of literature method and verified by IR spectroscopy.[1] Other reactants and solvents were obtained from commercial sources and used for the reactions without further purification. Powder XRD patterns were obtained using a RIGAKU-Miniflex II diffractometer with Cu $K\alpha$ radiation (λ = 1.54056 Å). IR spectra were recorded on PerkinElmer Spectrum One FT-IR infrared spectrophotometer with pressed KBr pellets in the range of 4000-400 cm^{-1}. Thermal analyses were performed in a dynamic air atmosphere with a heating rate of 10 ^{o}C/min, using a NETZSCH STA 449C thermal analyzer. UV-vis spectra were performed on a SHIMADZU UV-2600 UV-visible spectrophotometer by using the same solvent as the blank. ICP analyses were conducted on an Ultima2 spectrometer. The crystal samples were vacuum dried at 80 °C for 24 h before ICP analysis. According to the TG curve, the loss of 3.2% between 30 and 80 °C correspomds to the loss of about seven water molecules per formula (calc. 3.08%). Therefore, the formula is $H_5K_3Na[Cu(en)_2]_2[Cu(en)_{0.75}(H_2O)_{2.5}]\{[(Te_2Nb_{19}O_{58})(\mu_3\text{-}OH)_2]\}\cdot16H_2O(C_{9.5}Cu_3K_3N_{9.5}NaNb_{19}O_{78.5}Te_2H_{82})$ for ICP analysis.

Proton conductivity experiments: Ac impedance measurements were carried out using a Zennium/IM6 impedance analyzer over the frequency range from 0.1 Hz to 5 MHz with an applied voltage of 50 mV. The relative humidity was controlled by a STIK Corp. CIHI-150B incubator. The sample was pressed to form a cylindrical pellet of crystalline powder sample (~1.5 mm thickness ×5 mm φ) coated with C-pressed electrodes. Two silver electrodes were attached to both sides of the pellet to form four end S3 terminals (quasi-four probe method). The bulk conductivity was estimated by semicircle fittings of Nyquist plots.

Synthesis of $H_5K_3Na[Cu(en)_2]_2[Cu(en)_{0.75}(H_2O)_{2.5}]\{[(Te_2Nb_{19}O_{58})(\mu_3\text{-}OH)_2]\}\cdot23H_2O$ (1): $K_7H(Nb_6O_{19})\cdot13H_2O$ (0.22 mmol, 300 mg), Na_2CO_3 (1.91 mmol, 202 mg), $Cu(CH_3COO)_2\cdot H_2O$ (1.00

mmol, 200 mg), TeO_2 (0.66 mmol, 105 mg), imidazole (0.73mmol, 50 mg) and en (0.2 mL) were dissolved in 8 mL H_2O, after stirring for 1 hour, the resulting mixture was sealed in a Teflon-lined autoclave (23 mL) and heated at 140 °C for 3 days. After cooling down to room temperature and filtering, a purple solution was obtained. Slow evaporation of the purple solution was continued, and purple block crystals were obtained after one month. Yield: about 25 % (based on $K_7H(Nb_6O_{19})\cdot 13H_2O$). ICP and elemental analyses (based on a dried sample) calcd (found %) for $C_{9.5}Cu_3K_3N_{9.5}NaNb_{19}O_{78.5}Te_2H_{82}$: K, 2.98 (3.88); Cu, 4.84 (5.04); Te, 6.48 (6.68); Nb, 44.84 (45.00). IR (KBr pellet, v/cm^{-1}) (Fig S14): 3243(m), 3134(m), 2892(w), 1592(s), 1462(s), 1036(s), 868(s), 676(w), 576(s), 470(w)

Synthesis Discussion： During the synthesis process, some key factors contribute to our compound. (1) The crystals can be obtained by increasing or decreasing the amount of TeO_2, and they have the same unit cell parameters with compound **1**. However, the crystal quality is the best when the amount of TeO_2 is 100 mg. (2) we did a large number of parallel experiments and found that compound **1** cannot be formed when Na_2CO_3 was substituted by Li_2CO_3, K_2CO_3 and Cs_2CO_3. This could be explained by the fact that the countercation's size, charge, symmetry and solubility all affect crystallization of **1**. (3) Since no analogous products were obtained when we tried to synthesize isostructural compounds using different heteroatom (SeO_2, GeO_2, As_2O_3, Sb_2O_3), we came to the conclusion that this is related to the unique coordination mode and Te-O bond length of TeO_3^{2-}.

Single-crystal structure analysis: Single-crystal X-ray diffraction data of **1** were collected on Bruker Apex Duo CCD diffractometer using a graphite-monochromatized Mo Kα radiation (λ = 0.71073 Å) operating at 175 K. The structure of **1** was solved through direct methods and refined by full-matrix least-squares refinements based on F^2 using the SHELX-2014 program package. All non-H atoms were located by successive difference Fourier syntheses and refined anisotropically. The H atoms of the free water molecules and the coordinated water molecule were included in the final refinement. The final formula of **1** was determined by combining single-crystal X-ray diffraction with the element analysis, thermogravimetric analysis and charge balance, where elemental analysis verifies the number of metal atoms determined by single crystal diffraction, thermogravimetric analysis calculates the amount of crystal water (the weight loss before 200°C can be attributed to the removal of crystal water, with 23 H_2O for **1**), and the charge balance calculates the number of H atoms is 5 that cannot be identified by single crystal diffraction data. Crystallographic data and structure refinements for **1** are summarized in Table S1. CCDC 2300780 contains supplementary crystallographic data for **1**. These data can be obtained free of charge from the Cambridge Crystallographic Data Centre via www.ccdc.cam.ac.uk/data_request/cif.

Section S2 Additional Table

Table S1 Crystal Data and Structure Refinement for **1**

	1
Empirical formula	$C_{9.5}Cu_3K_3N_{9.5}NaNb_{19}O_{85.5}Te_2H_{96}$
Formula weight	4063.22
Crystal system	Monoclinic
Space group	*C*2/*c*
a (Å)	28.108(9)
b (Å)	15.854(5)
c (Å)	25.997(8)
α (°)	90
β (°)	104.516(4)
γ (°)	90
V (Å^3)	11215(6)
Z	4
F(000)	7484
ϑ range / °	1.487 to 25.021
limiting indices	$-33 \leq h \leq 33$
	$-16 \leq k \leq 18$
	$-30 \leq l \leq 30$
ρ_{calcd}(g cm^{-3})	2.359
Temperature (K)	175(2)
μ(mm^{-1})	3.138
Refl. Collected/unique	28294/9807

Data/restraints	9807/775
Parameters	636
R_{int}	0.0415
GOF on F^2	1.036
Final R indices (I= $2\sigma(I)$)	$R_1 = 0.0630$, $wR_2 = 0.1675$
R indices (all data)	$R_1 = 0.0717$, $wR_2 = 0.1735$

${}^{a}R_1 = \Sigma||F_o| - |F_c||/\Sigma|F_o|$, ${}^{b}wR_2 = [\Sigma w(F_o^2 - F_c^2)^2/w(F_o)^2]^{1/2}$, $w = 1/[\sigma^2(F_o^2) + (xP)^2 + yP]$, $P = (F_o^2 + 2F_c^2)/3$

Table S2 BVS calculations of the Nb, Te and Cu atoms.

Atoms	*Calcd*	*Oxidation state*	*Atoms*	*Calcd*	*Oxidation state*
Nb1	**5.00**	***Nb^{5+}***	**Nb2**	**4.91**	***Nb^{5+}***
Nb3	**5.11**	***Nb^{5+}***	**Nb4**	**5.03**	***Nb^{5+}***
Nb5	**5.06**	***Nb^{5+}***	**Nb6**	**5.03**	***Nb^{5+}***
Nb7	**4.98**	***Nb^{5+}***	**Nb8**	**5.13**	***Nb^{5+}***
Nb9	**5.05**	***Nb^{5+}***	**Nb10**	**5.00**	***Nb^{5+}***
Cu1	**2.06**	***Cu^{2+}***	**Cu2**	**2.16**	***Cu^{2+}***
Te1	**4.15**	***Te^{4+}***			

Table S3 BVS calculations of the O atoms.

Atoms	*Calcd*	*Oxidation state*	*Atoms*	*Calcd*	*Oxidation state*
O1	**1.79**	***O^{2-}***	**O2**	**1.61**	***O^{2-}***
O3	**1.95**	***O^{2-}***	**O4**	**1.08**	***OH^{-}***
O5	**2.10**	***O^{2-}***	**O6**	**1.82**	***O^{2-}***
O7	**1.91**	***O^{2-}***	**O8**	**2.13**	***O^{2-}***
O9	**1.81**	***O^{2-}***	**O10**	**1.90**	***O^{2-}***

O11	**1.71**	O^{2-}	**O12**	**1.74**	O^{2-}
O13	**1.50**	O^{2-}	**O14**	**1.89**	O^{2-}
O15	**1.93**	O^{2-}	**O16**	**1.55**	O^{2-}
O17	**1.80**	O^{2-}	**O18**	**1.76**	O^{2-}
O19	**1.84**	O^{2-}	**O20**	**2.02**	O^{2-}
O21	**1.57**	O^{2-}	**O22**	**1.56**	O^{2-}
O23	**1.65**	O^{2-}	**O24**	**1.62**	O^{2-}
O25	**1.64**	O^{2-}	**O26**	**1.54**	O^{2-}
O27	**1.98**	O^{2-}	**O28**	**1.63**	O^{2-}
O29	**1.89**	O^{2-}	**O30**	**1.77**	O^{2-}

Table S4 Elemental analysis data for **1**

Sample		*K*	*Cu*	*Nb*	*Te*
1	Calcd. (%)	2.98	4.84	44.84	6.48
	Found. (%)	3.88	5.04	45.00	6.68

Table S5 The caculation of the activation energy (E_a) of **1**

T/K	1000/T	R/Ω	σ/ S cm^{-1}	lnσT	*slope*	E_a
298.15	3.35	19833	3.9×10^{-5}	-5.98	-11.4	E_a = 0.97 eV
308.15	3.25	8170.7	9.4×10^{-5}	-4.19		
318.15	3.14	2360.8	3.2×10^{-4}	-2.42		
328.15	3.05	752.12	1.0×10^{-3}	-1.83		
338.15	2.96	301.18	2.5×10^{-3}	-1.50		
348.15	2.87	103.97	7.3×10^{-3}	-1.18		
358.15	2.79	96.824	7.9×10^{-3}	-0.62		

Table S6 Summary of proton conductivity of PONbs

Compounds	σ	E_a	Conditions	Ref.
$H_6K_4(H_2O)_{10}[Cu(en)_2]_2\{[(Te_2Nb_{19}O_{60})(\mu_3\text{-}OH)][Cu(H_2O)_4)]\}\cdot 7H_2O$	7.9×10^{-3} S cm^{-1}	0.97 eV	85 °C 98% RH	This work
$[Na_2(H_2O)_9]_2\{[Na_4K_6(H_2O)_{10}][Cr_{2.5}Nb_{27.5}O_{66}(OH)_{20}(H_2O)_2]_2\}\cdot nH_2O$	6.4×10^{-2} S cm^{-1}	0.96 eV	70 °C 98% RH	2
$H_{12}\{[Cu(en)_2]_{10}[Nb_{68}O_{182}(OH)_8(H_2O)_{10}]\}\cdot 54H_2O$	5.71×10^{-3} S cm^{-1}	1.02 eV	85 °C 98% RH	3
$H_{12}\{[Cu(en)_2]_6[Nb_{68}O_{176}(OH)_{12}(H_2O)_{12}]\}\cdot 52H_2O$	5.25×10^{-3} S cm^{-1}	1.04 eV	85 °C 98% RH	3
$K_6[Cu(en)_2]_{20}H_{72}[Dy_{14}Nb_{192}]\cdot$Solvents	3.75×10^{-3} S cm^{-1}	0.55 eV	85 °C 98% RH	4
$K_2Na_2H_{16}(H_2O)_4[Cu(en)_2]_2[Cu(en)_2(H_2O)]_4\{[Cu(en)_2]_6[SiNb_{18}O_{54}]_3\}\cdot 34H_2O$	3.48×10^{-3} S cm^{-1}	0.50 eV	70 °C 98% RH	5
$H_4[Cu(en)_2]_4\{K_4(H_2O)_2[Cu(en)_2]_5[Cu_5(trz)_2(en)_4(OH)_2][Dy_2Cu_2(en)_2(CO_3)_3(H_2O)_2(OH)_3][Dy(H_2O)_4][DyNb_{23}O_{68}(H_2O)_4]_2\}\cdot 60H_2O$	3.42×10^{-3} S cm^{-1}	1.03 eV	85 °C 98% RH	6
$H_{20}[Cu(en)_2]_4\{[Cu(en)_2]_4[Dy_2(C_2O_4)(H_2O)_4]_2[(Nb_{32}(OH)_4(H_2O)_3O_{89}]_2\}\cdot 54H_2O$	7.15×10^{-4} S cm^{-1}	0.80 eV	85 °C 98% RH	6
$H_9[Cu(en)(H_2O)_2][Cu(en)_2]_8[Dy(H_2O)_4]_3[Nb_{24}O_{69}(H_2O)_3]_2\cdot 36H_2O$	2.14×10^{-3} S cm^{-1}	0.91 eV	85 °C 98% RH	7
$H_9K[Cu(en)_2(H_2O)]_5[Cu(en)_2]_4[Eu(H_2O)_4]_3[Nb_{24}O_{69}(H_2O)_3]_2\cdot 2en\cdot 45H_2O$	1.50×10^{-3} S cm^{-1}	0.55 eV	85 °C 98% RH	7
$H_9[Cu(en)_2(H_2O)_2][Cu(en)_2]_{12}[In(en)]_5[Nb_{23}O_{65}(OH)_3(H_2O)_2]\{Nb_{24}O_{67}(OH)_2(H_2O)_3]_2\}\cdot 68H_2O$	1.78×10^{-3} S cm^{-1}	0.67 eV	85 °C 98% RH	8
$H_5[Cu(H_2O)(en)_2]_2[Cu(H_2O)_2(en)_2]\{[Cu(en)_2(H_2O)]_2Eu(H_2O)_3Te_6Nb_{18}O_{64}(OH)_4\}\cdot 7H_2O$	1.66×10^{-3} S cm^{-1}	0.92 eV	85 °C 98% RH	9
$[Cu(en)_2(H_2O)]_2\{[Cu(en)]_4[Cu(en)_2]_5\}$	1.35×10^{-3}	1.27 eV	85 °C	10

$\{[Cu(en)_2KNb_{24}O_{72}H_{10}]_2\}\cdot 6en\cdot 70H_2O$	S cm^{-1}		98% RH	
$\{[Cu(en)_2]@\{[Cu_2(en)_2(trz)_2]_6(Nb_{68}O_{188})\}\}$	1.30×10^{-3} S cm^{-1}	0.54 eV	85 °C 98% RH	11
$H_6[Cu(en)_2]_8[Ge_{12}O_6(OH)_8Nb_{38}O_{120}]\cdot 34H_2O$	3.04×10^{-4} S cm^{-1}	0.61 eV	85 °C 98% RH	12
$H_8[Cu(en)_2]_7[Ge_{12}O_8(OH)_4Nb_{38}O_{120})]\cdot 28H_2O$	1.62×10^{-4} S cm^{-1}	0.47 eV	85 °C 98% RH	12
$K_2H[Cu(phen)(H_2O)]_4[Cu(phen)]_2$ $[(LiNb_8Te_4O_{40})]\cdot 34H_2O$	1.50×10^{-3} S cm^{-1}	1.46 eV 0.47 eV	85 °C 98% RH	13

Section S3 Additional Figures

Fig. S1 The crystal morphology of compound **1** under an optical microscope.

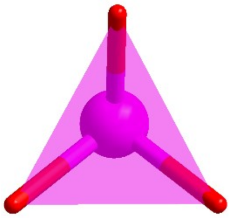

Fig. S2 The coordination modes of TeO_3^{2-} anion.

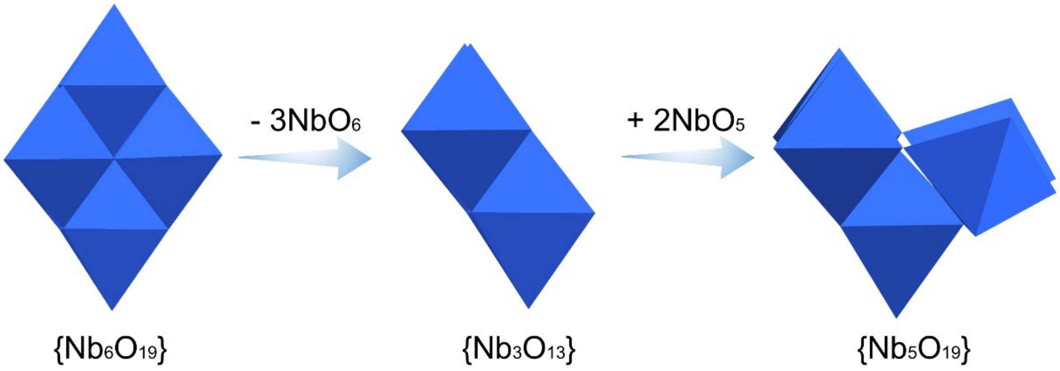

Fig. S3 The schematic diagram of the $\{Nb_5O_{19}\}$.

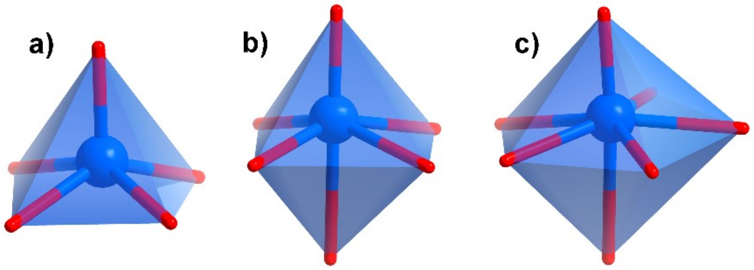

Fig. S4 The coordination environments of Nb^{5+} in **1**: a) penta-coordinated tetragonal pyramid; b) hexa-coordinated octahedron; c) hepta-coordinated pentagonal bipyramid.

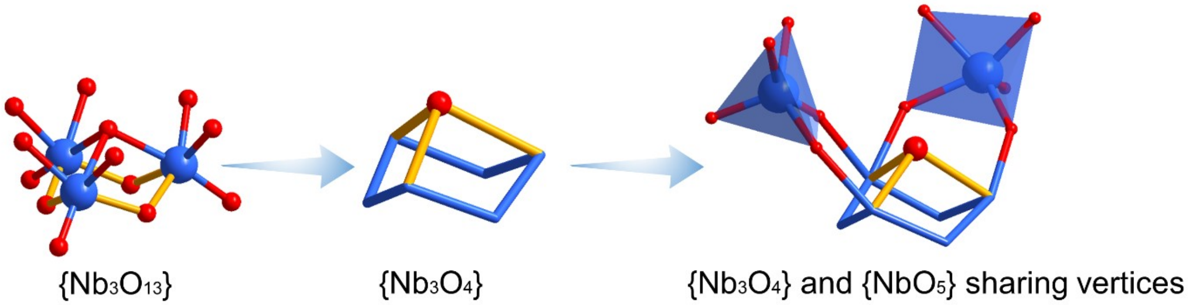

Fig. S5 The schematic diagram of chair-like configuration for $\{Nb_3O_4\}$.

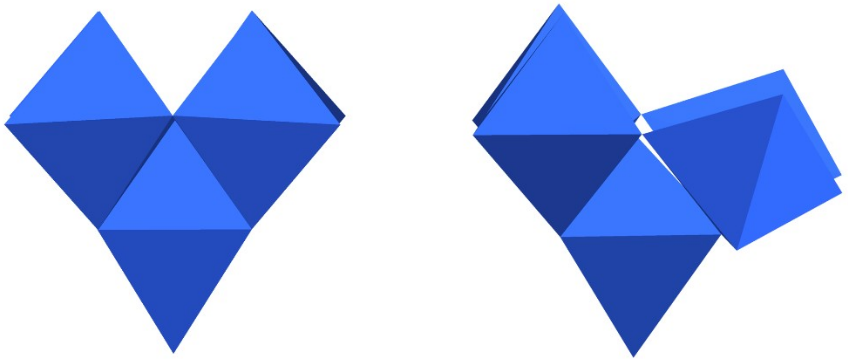

Fig. S6 The structure comparison diagram of classical $\{Nb_5O_{18}\}$ and $\{Nb_5O_{19}\}$ in **1**.

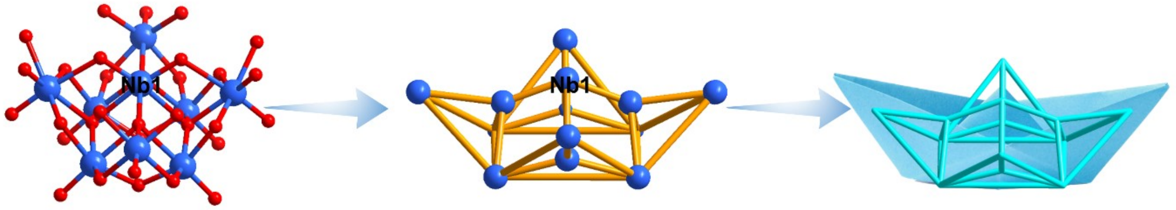

Fig. S7 The structure of boat-shaped {Nb_9O_{32}} cluster.

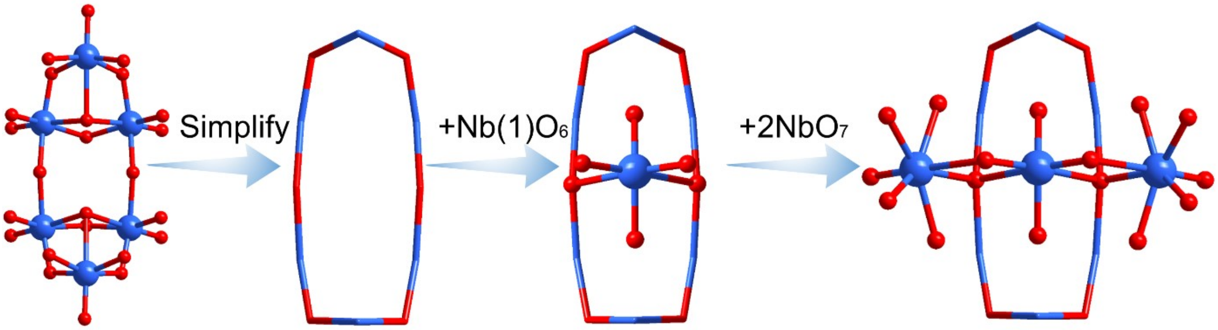

Fig. S8 The hull schematic diagram of the boat-shaped.

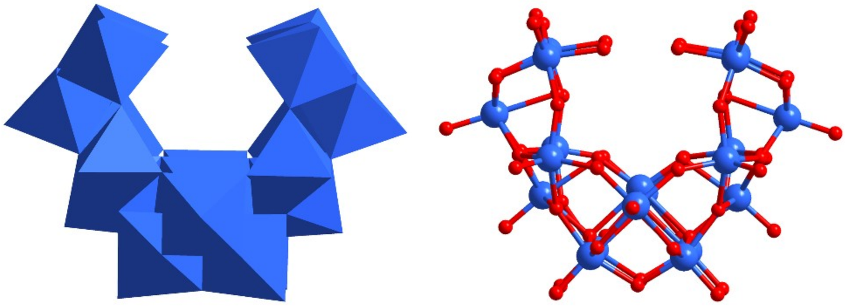

Fig. S9 The structures of nest-like {$Nb_{19}O_{58}$} cluster.

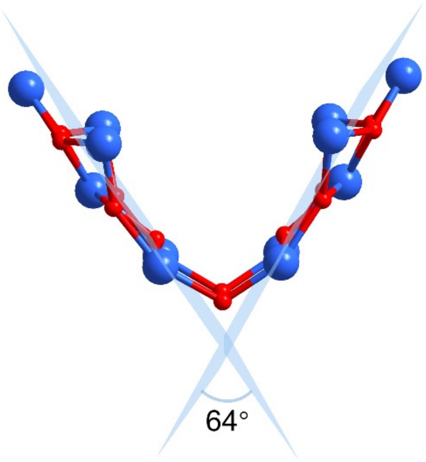

Fig. S10 The angle between two pentagonal {(Nb)Nb_5}.

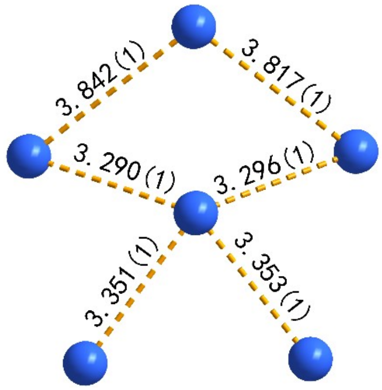

Fig. S11 The distances between adjacent Nb atoms.

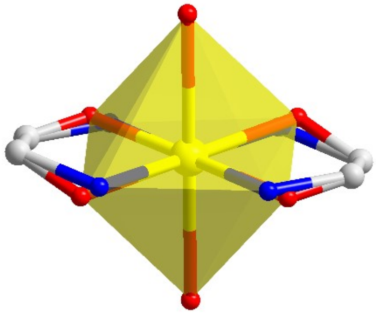

Fig. S12 The coordination environment of Cu^{2+} in $[Cu(H_2O)_{2.5}(en)_{0.75}]$.

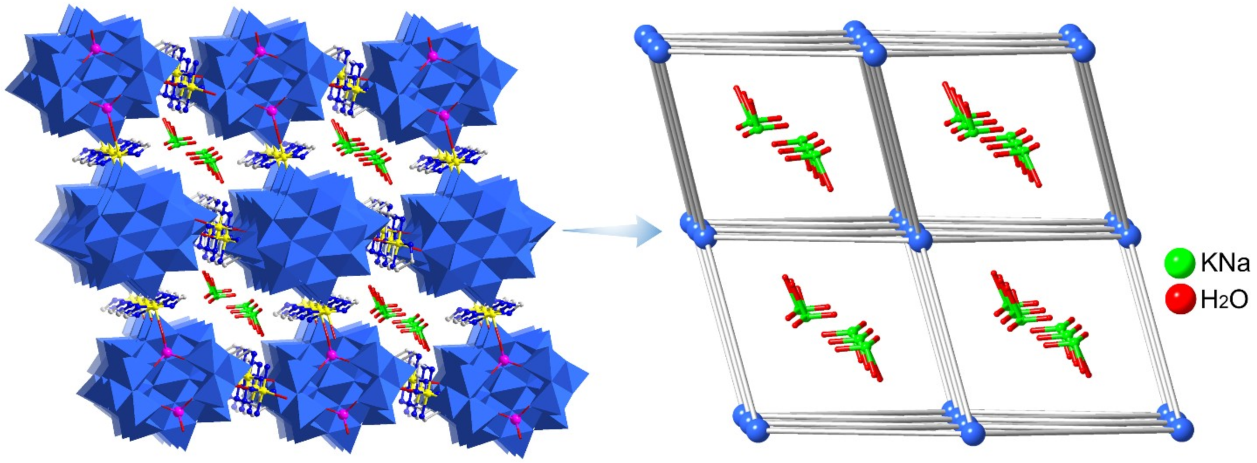

Fig. S13 View of the three-dimensional framework structure with K^+/Na^+ cations situated in the channels.

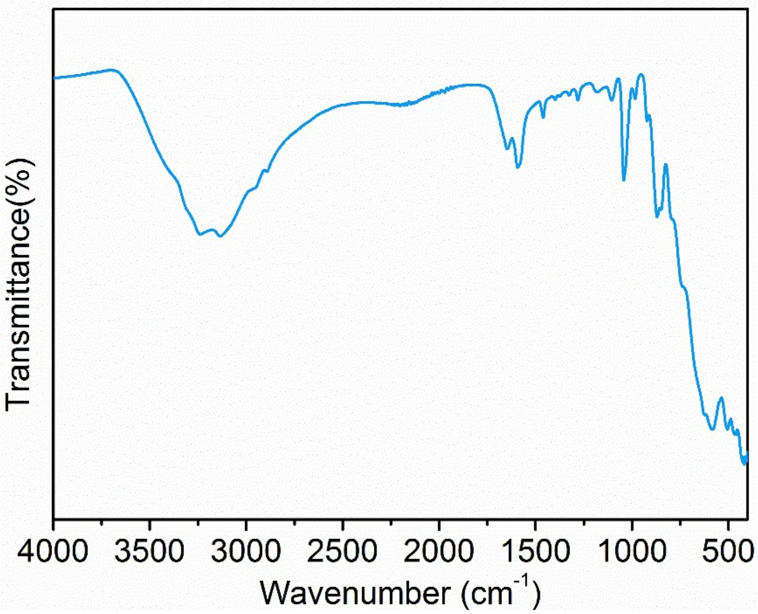

Fig. S14 The infrared spectrum of **1**

In the IR spectrum, the broad peak at 3243 cm^{-1} is attributed to the ν(O-H) stretching vibration of water. The ν(C-H) and ν(N-H) stretching vibrations appear at about 3134 cm^{-1} and 2892 cm^{-1} and their bending vibrations peak appear at about 1100 cm^{-1} and 1600 cm^{-1}. The absorption peak at about 1036 cm^{-1} can be attributed to the stretching vibration peak of C-N. The peaks that appear in the range of 400 to 1000 cm^{-1} can be attributed to the characteristic absorption peak of Nb-O, of which 868 cm^{-1} is the stretching vibration peak of ν(Nb-O$_t$) and 676 cm^{-1} and 470 cm^{-1} are the stretching vibration peaks of ν(Nb-O$_b$-Nb).

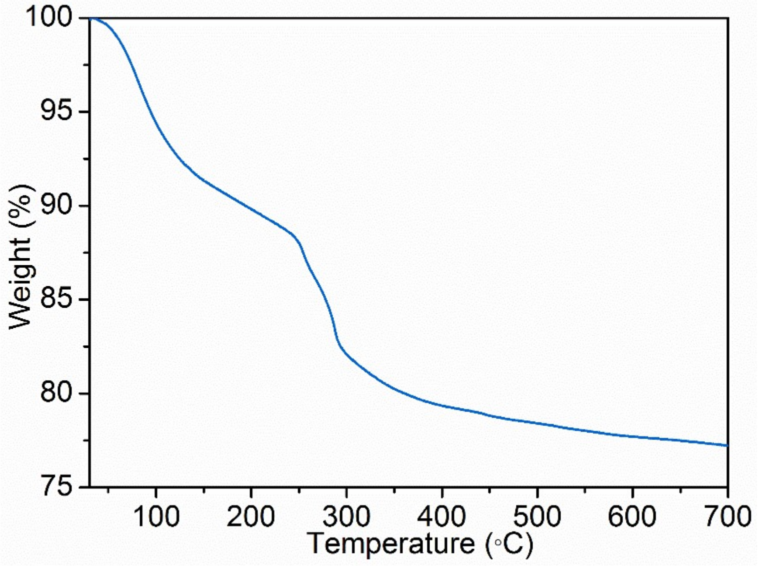

Fig. S15 The TG curve of **1**

The thermal stability of **1** was determined by thermogravimetric analysis at a heating rate of 10 °C/min in an argon atmosphere from 30 °C to 700 °C. As shown in Fig. S15, **1** has a continuous weight loss process in the temperature range of 30 °C to 700 °C. The initial weight loss of 10.18% from 30 to 200 °C corresponds to the approximately 23 lattice water molecules per formula (calc. 10.57%). After 200 °C , compound **1** begins to decompose and converts to oxide.

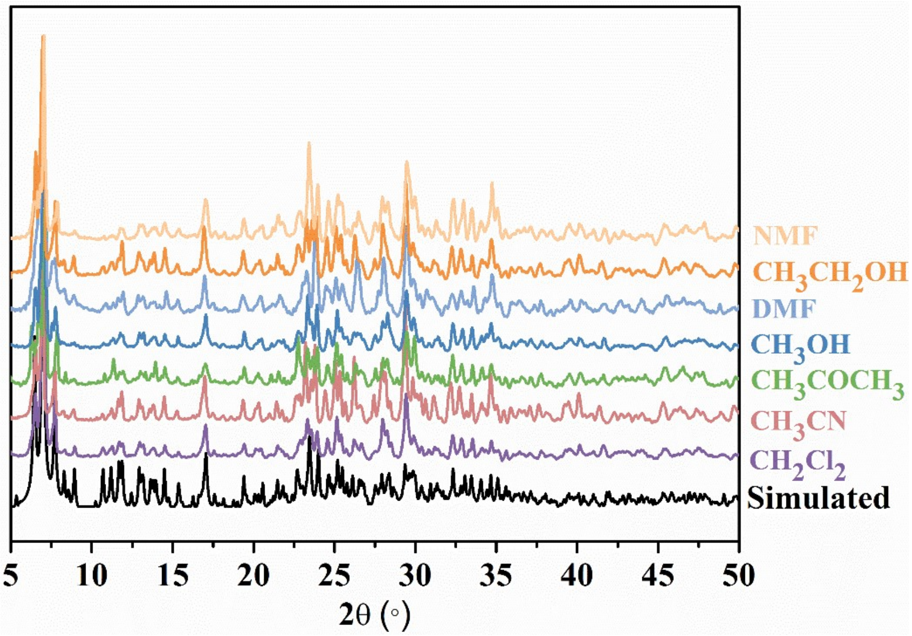

Fig. S16 Simulated PXRD patterns and experimental PXRD pattern of **1** soaked in different organic solvents for 24 hours.

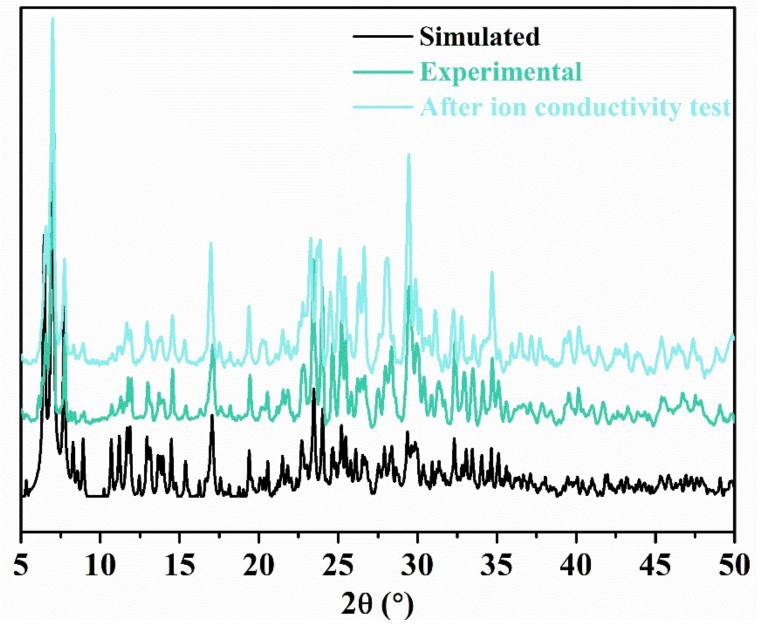

Fig. S17 Simulated PXRD patterns and experimental PXRD pattern of **1** after proton conductivity test.

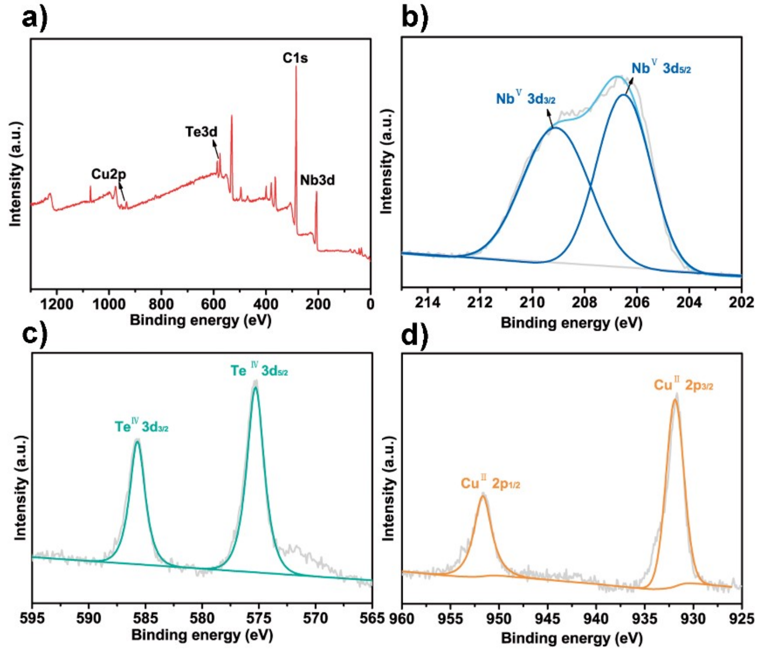

Fig. S18 The XPS spectra of **1** after proton conductivity test.

Table S7 proton conductivity of **1** from 25 to 85 °C and at 55% RH

T/K	1000/*T*	*R*/Ω	*σ*/ S cm^{-1}
298.15	3.35	61967	1.2 × 10^{-5}
308.15	3.25	26903	2.8 × 10^{-5}
318.15	3.14	9629.4	7.9 × 10^{-5}
328.15	3.05	4670.3	1.6 × 10^{-4}
338.15	2.96	3574.8	2.1 × 10^{-4}
348.15	2.87	1971.3	3.9 × 10^{-4}
358.15	2.79	1535.2	5.0 × 10^{-4}

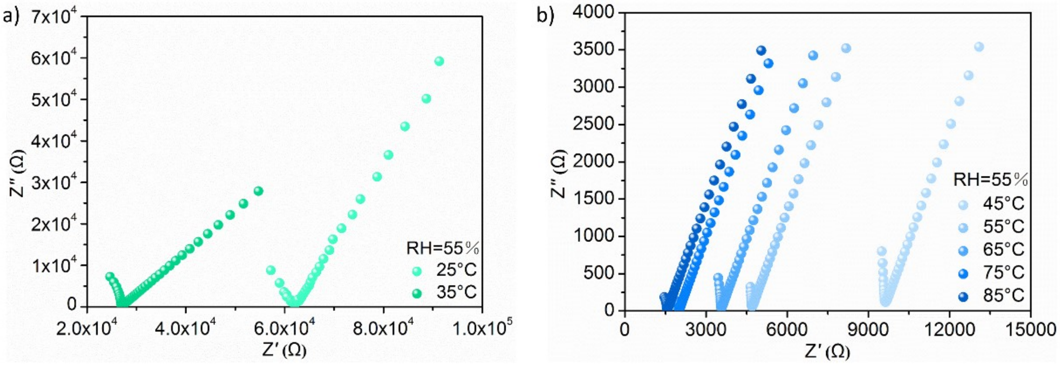

Fig. S18 Nyquist plot for **1** at different temperatures with 55% RH.

The temperature-dependent proton conductivity behavior was measured at temperatures ranging from 25 to 85 °C and at 55% RH. As shown in Fig. S18, when the temperature was increased from 25 to 85° C, the σ value rose continuously and reached a maximum of 5.0× 10^{-4}S cm^{-1} at 55% RH.

Section S4 Topology analysis

Topology for Nb1

Atom Nb1 links by bridge ligands and has

```
Common vertex with                          R(A-A)
Nb 1    0.5000    0.7605    0.7500   ( 1 1 1)    15.402A       1
Nb 1    0.5000    0.7605   -0.2500   ( 1 1 0)    15.402A       1
Nb 1    1.0000    0.7395    0.2500   ( 1 0 0)    16.135A       1
Nb 1    1.0000   -0.2605    0.2500   ( 1-1 0)    16.135A       1
Nb 1    0.0000    0.7395    0.2500   ( 0 0 0)    16.135A       1
Nb 1    0.0000   -0.2605    0.2500   ( 0-1 0)    16.135A       1
------------------------
Structural group analysis
------------------------

------------------------
Structural group No 1
------------------------
Structure consists of 3D framework with Nb

Coordination sequences
----------------------
Nb1:  1  2  3   4   5   6   7   8    9   10
Num   6 18 38  66 102 146 198 258  326  402
Cum   7 25 63 129 231 377 575 833 1159 1561
----------------------
TD10=1561

Vertex symbols for selected sublattice
--------------------------------------
Nb1 Point symbol:{4^12.6^3}
Extended point symbol:[4.4.4.4.4.4.4.4.4.4.4.4.6(4).6(4).6(4)]
--------------------------------------
Point symbol for net: {4^12.6^3}
6-c net; uninodal net

Topological type: pcu alpha-Po primitive cubic; 6/4/c1; sqc1 (topos&RCSR.ttd) {4^12.6^3} - VS
[4.4.4.4.4.4.4.4.4.4.4.4.*.*.*] (72442 types in 11 databases)

Elapsed time: 4.67 sec.
```

Section S5 References

1. R. P. Bontchev, E. L. Venturini and M. Nyman, *Inorg. Chem.*, 2007, **46**, 4483–4491.

2. Z. W. Guo, Y. Chen, D. Zhao, Y. L. Wu, L. D. Lin, S. T. Zheng, A Chromium-Substituted Polyoxoniobate with High Proton Conductivity. *Inorg. Chem*. 2019, **58**, 4055-4058.

3. Y.-D. Lin, Z.-K. Zhu, R. Ge, H. Yu, Z. Li, C. Sun, Y.-Q. Sun, X.-X. Li, S.-T. Zheng, Proton conductive polyoxoniobate frameworks constructed from nanoscale {Nb68O200} cages. *Chem. Commun*. 2021, **57** , 4702-4705.

4. R. D. Lai, J. Zhang, X. X. Li, S. T. Zheng, G. Y. Yang, Assemblies of Increasingly Large LnContaining Polyoxoniobates and Intermolecular Aggregation-Disaggregation Interconversions. *J. Am. Chem. Soc*. 2022, **144**, 19603-19610.

5. Y. Y. Lin, J. Zhang, Z. K. Zhu, Y. Q. Sun, X. X. Li, S. T. Zheng, An ultrastable {$SiNb_{18}O_{54}$}- based hybrid polyoxoniobate framework for selective removal of crystal violet from aqueous solution and proton-conduction. *Inorg. Chem. Commun*. 2020, **113**. 107766.

6. R. D. Lai, Z. K. Zhu, Y. L. Wu, Y. Q. Sun, C. Sun, X. X. Li, S. T. Zheng, Proton-Conductive Polyoxometalate Architectures Constructed from Lanthanide-Incorporated Polyoxoniobate Cages. *Inorg. Chem*. 2022, **61**, 21047-21054.

7. J. Zhang, R. D. Lai, Y. L. Wu, Z. K. Zhu, Y. Q. Sun, Q. X. Zeng, X. X. Li, S. T. Zheng, High-dimensional Polyoxoniobates Constructed from Lanthanide-incorporated High-nuclear {$[Ln(H_2O)_4]_3[Nb_{24}O_{69}(H_2O)_3]_2$} Secondary Building Units. *Chem. – Asian J.* 2020, **15**, 1574- 1579.

8. H. Yu, Y.-D. Lin, Z.-Y. Liu, Y.-Q. Sun, Y.-Q. Zheng, A Three-Dimensional (3D) Indium Containing Polyoxoniobate Framework Based on $\{In_5Nb_{71}\}_n$ Helical Pillars. *Inorg. Chem*. 2022, **61**, 8112-8116.

9. R. D. Lai, H. L. Feng, Y. Q. Sun, X. X. Li, S. T. Zheng, A lanthanide-tellurium heterometal encapsulated sandwich-type heteropolyoxoniobate with a 3D pcu-type hydrogen-bonded network. *Dalton Trans.* 2022, **51**, 10571-10577.

10. Z. K. Zhu, L. D. Lin, J. Zhang, X. X. Li, Y. Q. Sun, S. T. Zheng, A rare 4-connected nebtype 3D chiral polyoxometalate framework based on $\{KNb_{24}O_{72}\}$ clusters. *Inorg. Chem. Front.* 2020, **7** , 3919-3924.

11. Z. K. Zhu, Y. Y. Lin, L. D. Lin, X. X. Li, Y. Q. Sun, S. T. Zheng, A Rare 3D Porous Inorganic-Organic Hybrid Polyoxometalate Framework Based on a Cubic Polyoxoniobate-Cupric Complex Cage with a High Water Vapor Adsorption Capacity. *Inorg. Chem*. 2020, **59** , 11925- 11929.

12. Y. J. Wang, L. Yu, X. X. Li, Y. Q. Sun, S. T. Zheng. Two Unprecedented Germanoniobate Frameworks Based on High-nuclearity Peanut-shaped $\{Ge_{12}Nb_{38}\}$ Clusters. *Inorg.Chem*. 2024, **63**, 1388−1394.

13. P. X. Wu, R. D. Lai, R. Ge, C. Sun, G. Q. W, X. X. Li, S.-T. Zheng, A Tellurium-Substituted Heteropolyniobate with Unique π–π Stacking and Proton Conduction Property. *Inorg.Chem*. 2021, **60**, 6162−6166.